ARTICLE NO. 78-1367

Re-entry Vehicle Dispersion from Entry Angular Misalignment

D.H. Platus*
The Ivan A. Getting Laboratories, The Aerospace Corporation, El Segundo, Calif.

An approximate solution is obtained for the dispersion of a re-entry vehicle caused by an initial angular misalignment between the vehicle axis of symmetry and the velocity vector at entry into the atmosphere. The dispersion depends on the exoatmospheric motion, which determines the precession mode of the lift vector during angle-of-attack convergence. Maximum dispersion results from an initial angular misalignment in absence of exoatmospheric coning motion. The trajectory deflection for this case occurs in a plane that leads the plane of initial angular misalignment by approximately 90 deg. The dispersion is approximately proportional to roll rate, in contrast to dispersion from body-fixed asymmetries, which varies inversely with roll rate.

Nomenclature

C_A = aerodynamic axial force coefficient
C_{L_θ} = aerodynamic lift force derivative
C_N = aerodynamic normal force coefficient
C_{N_θ} = aerodynamic normal force derivative
CR = cross-range dispersion
d = aerodynamic reference diameter
h = altitude
h_0 = entry altitude
h_l = altitude of trajectory deflection
H = scale height for exponential atmosphere
I = pitch or yaw moment of inertia
I_x = roll moment of inertia
k_x = radius of gyration in roll
K = $2Hp_r/\mu \sin\gamma$
l = characteristic length, I/mx_{st}
L = lift force
m = vehicle mass
M = pitch moment
$M_{\dot\theta}$ = pitch damping moment
$M_{\dot\psi}$ = yaw damping moment
p = roll rate
p_r = reduced roll rate, $\mu p/2$
S = aerodynamic reference area
t = time
u = vehicle velocity
u_0 = entry velocity
V = dispersion velocity, $v+iw$
v,w = components of V
x = $\sqrt{1+\xi}$
x_l = value of x at trajectory deflection
x_{st} = static margin
z = altitude variable
γ = path angle
θ = angle of attack (Euler angle)
θ_0 = entry angle of attack
$\dot\theta$ = pitch rate
μ = I_x/I
ξ = ω^2/p_r^2
ρ = atmospheric density
ρ_0 = reference value of atmospheric density
ρ_l = atmospheric density at trajectory deflection altitude
ϕ = roll angle (Euler angle)
ψ = precession angle (Euler angle)
$\dot\psi$ = precession rate
$\dot\psi_{+,-}$ = precession modes
ω = undamped natural pitch frequency

Presented as Paper 78-1367 at the AIAA Atmospheric Flight Mechanics Conference, Palo Alto, Calif., Aug. 7-9, 1978; submitted Sept. 1, 1978; revision received Jan. 12, 1979.

Index categories: Entry Vehicle Dynamics and Control; LV/M Trajectories and Tracking Systems; LV/M Dynamics and Control.

*Senior Scientist, Aerophysics Laboratory. Associate Fellow AIAA.

Introduction

ONE of several sources of ballistic re-entry vehicle dispersion occurs during separation of the re-entry vehicle from the boost vehicle, which results in an angular misalignment between the vehicle axis of symmetry and the velocity vector at entry. This initial angle of attack causes lift as the vehicle traverses the atmosphere and can result in dispersion from lift nonaveraging. The resulting impact error is small relative to error from other known sources.[1] Under certain conditions, the error could become more significant. The sensitivity to various parameters is derived herein. The dispersion depends on the manner in which the lift vector and its rate of rotation in space (precession rate) are coupled during the initial re-entry motion.[2] It has been shown that there are two precession modes that comprise the familiar epicyclic motion of an axially symmetric missile in untrimmed flight.[3] Limiting cases of the two precession modes correspond with specific deployment conditions during boost vehicle separation. The negative precession mode, which results from an initial angle of attack in absence of exoatmospheric coning motion, results in significantly greater dispersion than the other limiting case of positive precession, in which the exoatmospheric precession cone is symmetric about the velocity vector. A simple closed-form solution obtained for the dispersion velocity for the negative precession case reveals the first-order influence of various parameters on the dispersion. The dispersion is relatively insensitive to most vehicle aerodynamic properties with the exception of static margin, and is independent of vehicle mass properties except for the radius of gyration in roll. The dispersion also varies directly with the roll rate, in contrast to lift nonaveraging dispersion from body-fixed asymmetries, which varies inversely with roll rate. Also significant is the observation that the trajectory deflection occurs in the first cycle of lift vector precession about the velocity vector and lies in a plane that leads the plane of the initial angular misalignment by approximately 90 deg. If the magnitude and direction of the misalignment angle is known, e.g., if the vehicle is aligned with the velocity vector at separation such that the entry angle of attack is determinable, this dispersion source can be partially compensated for in the targeting model.

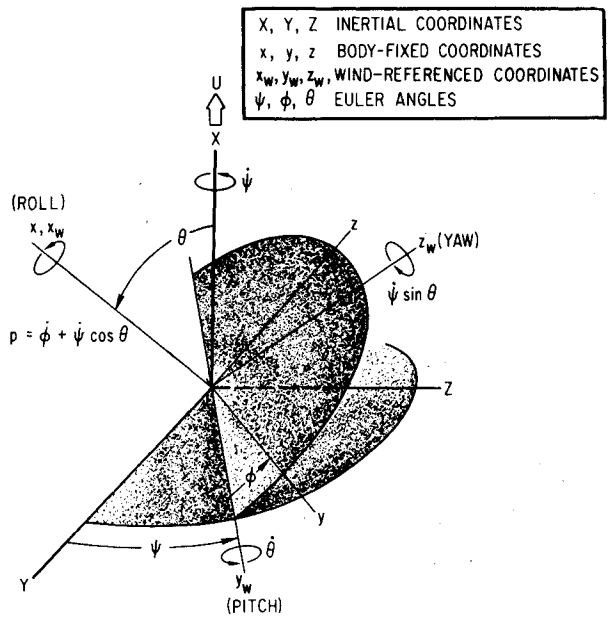

Fig. 1 Euler angle coordinates.

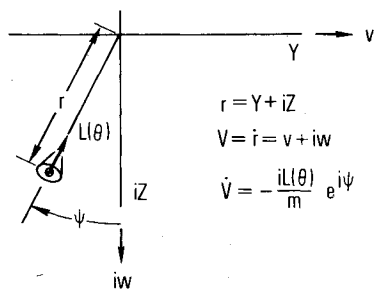

Fig. 2 Transverse velocity.

Analysis

Cross-range dispersion of a spinning missile can be described by the relation (Figs. 1 and 2)[2]

$$V(t) \cong V(0) - \frac{i}{m}\int_0^t L(\theta)\exp(i\psi)\,dt \tag{1}$$

where $V(t)$ is the missile transverse velocity in the cross plane, $L(t)$ is the lift force, which is dependent on the angle of attack θ, and ψ is the precession angle of the lift vector in the cross plane. Lateral velocities are small enough so that the pitch angle θ in the classical Euler angle system is, for practical purposes, the total angle of attack. For a symmetric missile with constant roll rate, the angles θ and ψ are described approximately by the moment equations of motion[3]:

$$\ddot{\theta} + \mu p\dot{\psi}\sin\theta - \dot{\psi}^2\sin\theta\cos\theta = \frac{M(\theta)}{I} + \frac{M_{\dot{\theta}}}{I}\dot{\theta} \tag{2}$$

$$\frac{d}{dt}(\dot{\psi}\sin\theta) + \dot{\theta}\dot{\psi}\cos\theta - \mu p\dot{\theta} = \frac{M_{\dot{\psi}}}{I}\dot{\psi}\sin\theta \tag{3}$$

$$p = \dot{\phi} + \dot{\psi}\cos\theta \tag{4}$$

where $M(\theta)$ is the static pitch moment, and $M_{\dot{\theta}}$ and $M_{\dot{\psi}}$ are rate damping moments. We consider first the case of a static moment only, and assume for $M(\theta)$ the form

$$M(\theta)/I = -\omega^2\sin\theta \tag{5}$$

where ω is the vehicle undamped natural pitch frequency. In absence of a yaw damping moment $M_{\dot{\psi}}$, Eq. (3) can be integrated to yield

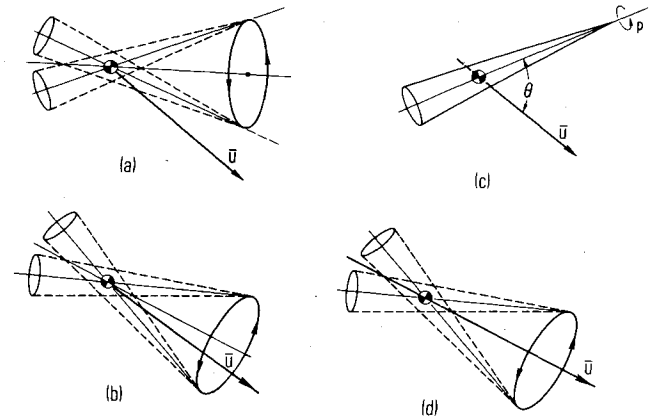

Fig. 3 Possible exoatmospheric motions: a) velocity vector outside exocone; b) velocity vector inside exocone; c) pointing error with zero lateral rate; d) symmetric coning about velocity vector.

$$\dot{\psi}\sin^2\theta + \mu p\cos\theta = \text{const} \tag{6}$$

Equation (6) is an expression of constancy of angular momentum about the velocity vector because there is no moment component in this direction in the classical Euler angle coordinates. For a rolling re-entry vehicle with initial angular misalignment θ_0, the constant in Eq. (6) is either $\mu p/\cos\theta_0$ or $\mu p\cos\theta_0$ for the limiting cases of positive ($\dot{\psi}_+$) or negative ($\dot{\psi}_-$) precession, respectively, and Eq. (6) can be written

$$\dot{\psi}_{+,-}\sin^2\theta = \mu p[(\cos\theta_0)^{\mp 1} - \cos\theta] \tag{7}$$

where the upper sign in the exponent corresponds to positive precession. Typical forms of entry angular motion are shown in Figs. 3a and 3b, and the two limiting case as $\theta \to \theta_0$ in Eq. (7) are shown in Figs. 3c and 3d for the positive and negative exponent, respectively. Positive precession about the velocity vector (clockwise looking forward, in the same direction as the roll rate) is initially at the exoatmospheric coning rate $\dot{\psi}_{+0} = \mu p/\cos\theta_0$. Negative precession (counterclockwise) is initially zero and results from the gyroscopic effect of the aerodynamic static moment acting on the spinning vehicle. The quasi-steady approximation $\ddot{\theta} = \dot{\theta} = 0$ in Eq. (2) is a good approximation to the initial angle-of-attack convergence of the circular coning motions, which, with Eq. (5), yields

$$\dot{\psi}_{+,-} = (p_r/\cos\theta)(1 \pm \sqrt{1 + \xi\cos\theta}) \tag{8}$$

where $p_r = \mu p/2$ and $\xi = \omega^2/p_r^2$. If we substitute $\dot{\psi}_{+,-}$ from Eq. (8) in Eq. (7), we obtain the relation

$$2\cos\theta(\cos\theta_0)^{\mp 1} = 1 + \cos^2\theta \pm \sqrt{1 + \xi\cos\theta}\sin^2\theta \tag{9}$$

which describes the quasisteady angle-of-attack convergence as a function of the static moment. With the small angle approximations $\sin\theta \approx \theta$, $\cos\theta \approx 1 - \theta^2/2$, Eqs. (8) and (9) reduce to the simple expressions for angle-of-attack convergence and precession rate, respectively, of circular coning motion in absence of damping[3]:

$$\theta/\theta_0 = (1 + \xi)^{-1/4} \tag{10}$$

$$\dot{\psi}_{+,-} = p_r(1 \pm \sqrt{1 + \xi}) \tag{11}$$

Equations (10) and (11) are compared with Eqs. (8) and (9) in Fig. 4 and are found to be good approximations, even for very large angles of attack. With these approximations, we can express the net transverse velocity from Eq. (1) in terms of

ξ as the independent variable with the use of the exponential atmosphere approximation

$$\rho(z) = \rho_0 \exp(z/H) \tag{12}$$

where z is measured downward from some initial reference altitude where the density is ρ_0, and H is a constant scale height. Assuming that the pitch frequency varies only with density over the altitude range of interest, and assuming a constant flight path angle, we obtain from the definition of ξ

$$\frac{d\xi}{\xi} = \frac{u \sin\gamma}{H} dt \tag{13}$$

The lift force per unit mass $L(\theta)/m$ in Eq. (1) can also be written in terms of ξ according to

$$L(\theta)/m = C_{L_\theta} qS\theta/m \approx \xi p_r^2 l\theta \tag{14}$$

where $l = I/mx_{st}$ is a characteristic length. Substitution of Eqs. (10), (13), and (14) in Eq. (1) yields, for the transverse velocity caused by initial angular misalignment,

$$V(\xi) = -\frac{ilHp_r^2\theta_0}{u \sin\gamma} \int_0^\xi (1+\xi)^{-1/4} \exp[i\Delta\psi(\xi)]\, d\xi \tag{15}$$

where $V(0) = 0$, and $\Delta\psi(\xi)$ is obtained on integrating $\dot{\psi}_{+,-}$ from Eq. (11) with the relation Eq. (13). It is expedient to make a further change of variable defined by

$$x = \sqrt{1+\xi} \tag{16}$$

which yields, for $V(x)$,

$$V(x) = -\frac{2ilHp_r^2\theta_0}{u \sin\gamma} \int_1^x \sqrt{x} \exp[i\Delta\psi(x)]\, dx \tag{17}$$

The precession rate, Eq. (11), expressed as a derivative with respect to the independent variable x with the use of Eqs. (13) and (16) can be written

$$\frac{d\psi_{+,-}}{dx} = -\frac{2Hp_r}{u \sin\gamma}\left(\frac{x}{x \mp 1}\right) \tag{18}$$

The negative precession rate can be integrated between the limits 1 to x to yield

$$\Delta\psi_-(x) = -K[\ln 2 - 1 + x - \ln(1+x)] \tag{19}$$

and the positive precession rate (because of the singularity at $x = 1$) can be integrated between the limits $1+\epsilon$ to x to yield†

$$\begin{aligned}\Delta\psi_+(x) &= \psi_+(x) - \psi_+(1+\epsilon) \\ &= K[x - 1 + \ln(x-1) - \epsilon - \ln\epsilon]\end{aligned} \tag{20}$$

where

$$K = 2Hp_r/u \sin\gamma \tag{21}$$

The complex transverse velocity, which determines the magnitude and direction of the trajectory deflection, is determined from the average value of the integral in Eq. (17) with appropriate integration limits depending on the precession mode. The integral is a function only of the constant K in the precession angle, Eq. (19) or (20), in addition to the independent variable x. As shown in Appendix

†Equation (17) is integrated between the same limits for the positive precession angle.

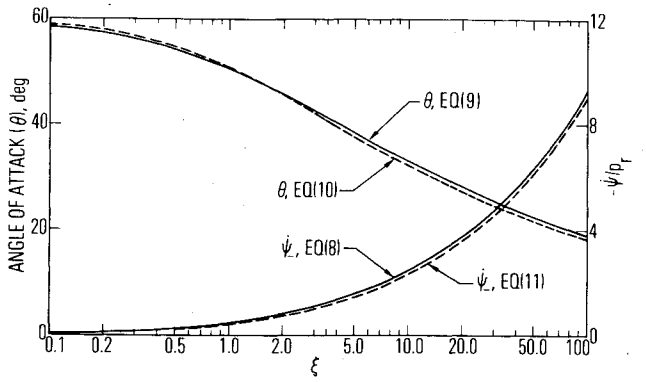

Fig. 4 Comparison of small-angle approximations for θ and $\dot{\psi}_-$ with exact, large-angle values for $\theta_0 = 60$ deg.

A, the nondimensional integral

$$\mathcal{I} = -iK \int_1^x \sqrt{x} \exp[i\Delta\psi(x)]\, dx \tag{22}$$

is only weakly dependent on K over a wide range of K of practical interest. The real and imaginary components of $\mathcal{I}$, obtained numerically, for various values of K with both positive and negative precession modes are shown in Figs. 5 and 6. The negative precession case results in appreciably greater dispersion, and the integral defined by Eq. (22) with the negative precession angle, Eq. (19), has an essentially constant average value $\mathcal{I} = -2.0$ over a wide range of K. If we substitute this value for Eq. (22) in Eq. (17), with the definition of K, Eq. (21), the net transverse velocity for negative precession is described by the simple expression

$$\overline{V}_- = -2lp_r\theta_0 = -I_x p\theta_0/mx_{st} = -k_x^2 p\theta_0/x_{st} \tag{23}$$

The latter form of Eq. (23) indicates that, to the first order, the trajectory deflection is a function only of the initial angle of attack, roll rate, radius of gyration in roll, and vehicle static margin. The net transverse velocity increment is in the negative real direction, which leads by 90 deg the plane of the initial angle of attack for the zero coning motion entry condition that results in negative precession. The trajectory deflection is directly proportional to roll rate in Eq. (23), in contrast to roll-trim dispersion of a spinning missile, in which the dispersion is inversely proportional to roll rate.[2]

The simple result, Eq. (23), is compared in Fig. 7 with an exact solution for the real component v of dispersion velocity during negative precession, obtained from a numerical integration of the equations of motion, Eqs. (2) through (5), for the vehicle and trajectory parameters listed below:

h_0	= 300 kft	I_x	= 1.15 slug-ft^2
u_0	= 23 kft/s	I	= 15 slug-ft^2
γ	= 30 deg	x_{st}	= 0.2 ft
m	= 8.703 slugs	C_A	= 0.1
d	= 1.5 ft	C_{N_θ}	= 1.9
S	= 1.767 ft^2	$C_N(\theta)$	= $C_{N_\theta} \sin\theta$
p	= 2 rps	θ_0	= 20 deg

An exact solution for the imaginary velocity component w is shown in Fig. 8. A standard atmosphere density distribution was utilized in the numerical evaluation, which in the altitude range of 220 to 300 kft, where the trajectory deflection occurs, is represented by an exponential scale height of approximately $H \approx 20$ kft. This gives a value of 1.68 for K. With the preceding vehicle and trajectory parameters, the transverse velocity from Eq. (23) is -2.90 ft/s, which compares with an average value of -2.60 ft/s for the velocity component v in Fig. 7. The small discrepancy is attributed to the

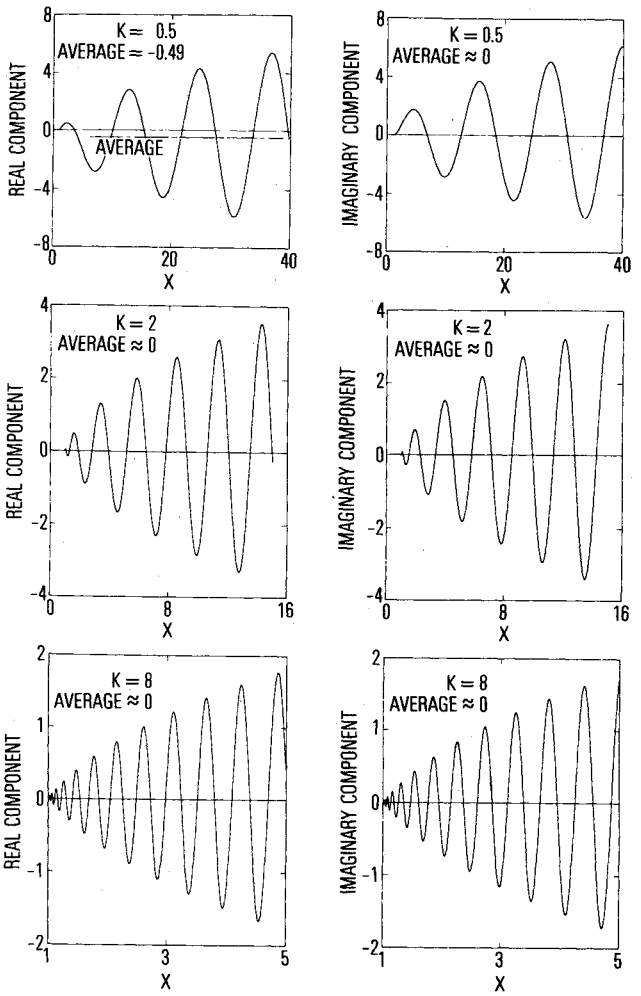

Fig. 5 Real and imaginary components of the intergral $\mathcal{I}$ with positive precession.

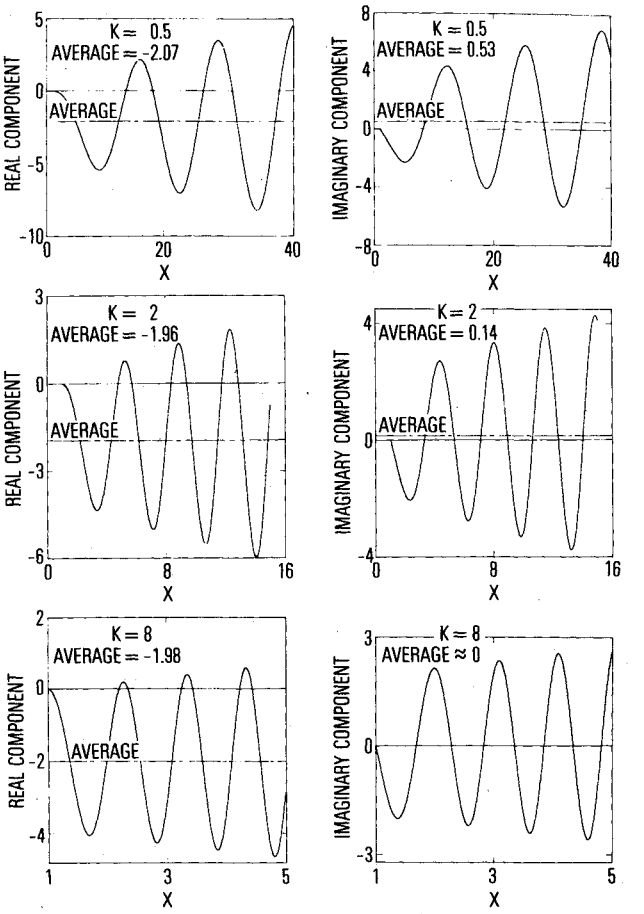

Fig. 6 Real and imaginary components of the integral $\mathcal{I}$ with negative precession.

small angle approximations used in the derivation of Eq. (23). We can account for larger angles of attack by including in the integrand of Eq. (22) the factor $C_{L_\theta}/C_{N_\theta}$, which is a function of the angle of attack defined approximately by

$$C_{L_\theta}/C_{N_\theta} = \cos\theta - C_A/C_{N_\theta} \tag{24}$$

If we express the angle of attack in terms of the independent variable x using Eqs. (10) and (16), then the correction to the integrand of Eq. (22) for $C_{L_\theta}/C_{N_\theta}$ is

$$C_{L_\theta}/C_{N_\theta} = \cos(\theta_0/\sqrt{x}) - C_A/C_{N_\theta} \tag{25}$$

Equation (22) was integrated with this correction for $K = 1.68$ corresponding to the aforementioned vehicle and trajectory parameters, and the average value was found to be -1.78 compared with -2.0 without the correction. This gives a net transverse velocity of -2.59 ft/s, which compares more favorably with the exact result of Fig. 7. With the small angle approximation of unity for the cosine term in Eq. (25), a slightly better appproximation to the dispersion velocity, Eq. (23), is given by

$$\overline{V}_- = -(I_x p\theta_0/mx_{st})(1 - C_A/C_{N_\theta}) \tag{26}$$

which yields -2.75 ft/s for the dispersion velocity of Fig. 7.

The cross-range impact dispersion CR is approximately equal to the product of the trajectory deflection angle and the path length from the point of trajectory deflection to impact. For a straightline trajectory with constant path angle γ, and with the net transverse velocity given by Eq. (23), the cross-range dispersion is

$$\mathrm{CR} \approx \frac{\overline{V}_- h_1}{u \sin\gamma} = \frac{I_x p\theta_0 h_1}{mx_{st} u \sin\gamma} \tag{27}$$

where h_1 is the altitude at which the net trajectory deflection occurs. We can obtain an approximate expression for h_1 from the observation that the net transverse velocity increment is reached when the lift vector rotates through the first quarter cycle for the negative precession case. From the definition of the independent variable x, Eq. (16), and the negative precession angle, $\Delta\psi_-(x)$, Eq. (19), the density ρ_1 at this altitude is

$$\rho_1 = \frac{p_r^2 I(x_1^2 - 1)}{C_{N_\theta} u^2 Sx_{st}} \tag{28}$$

where

$$\ell n[(x_1 + 1)/2] - x_1 \approx -\pi/2K - 1 \tag{29}$$

Again, using the exponential atmosphere approximation, we obtain, for h_1, in terms of an arbitrary entry altitude h_0, where the density is ρ_0

$$h_1 = h_0 - H\,\ell n\left[\frac{p_r^2 I(x_1^2 - 1)}{\rho_0 C_{N_\theta} u^2 Sx_{st}}\right] \tag{30}$$

which gives, for CR, the parametric relation

$$\mathrm{CR} \approx \frac{\theta_0 IK}{mHx_{st}}\left\{h_0 - H\,\ell n\left[\frac{K^2(x_1^2 - 1)I\sin^2\gamma}{4\rho_0 H^2 C_{N_\theta} Sx_{st}}\right]\right\} \tag{31}$$

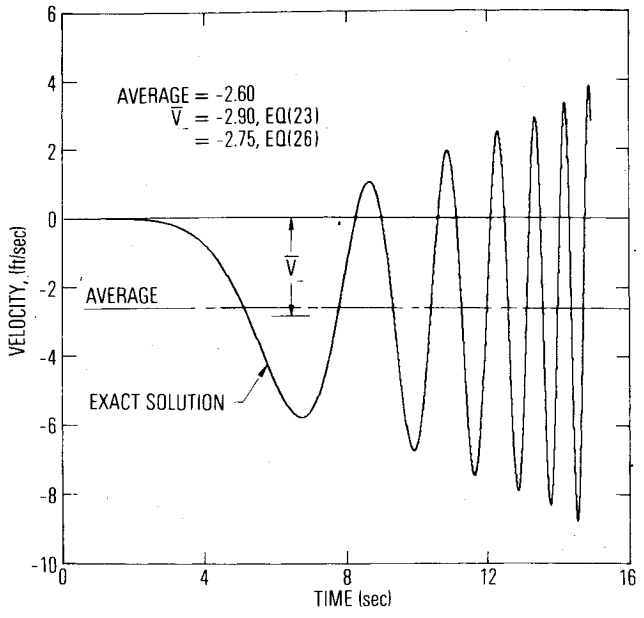

Fig. 7 Comparison of approximation for dispersion velocity with exact value obtained from numerical integration of equations of motion.

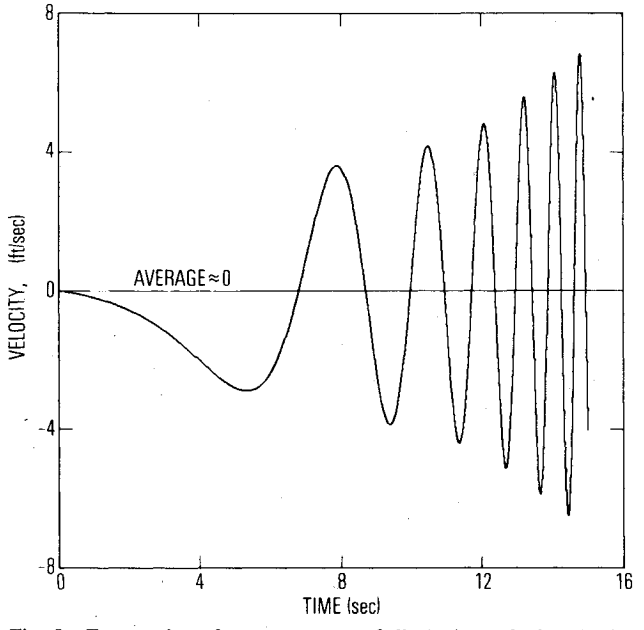

Fig. 8 Exact value of *w*-component of dispersion velocity obtained from numerical integration of equations of motion.

with x_l defined by Eq. (29). The altitude h_l is shown in Table 1 for a range of K values and is relatively insensitive to K. Also shown is the cross-range dispersion per unit angle of attack θ_0. Hence, the parametric dependence of the cross-range dispersion is described to the first order by the multiplier of h_l in Eq. (27).

Aerodynamic damping was excluded from the equations of motion, Eqs. (2) and (3), in the foregoing discussion. In Appendix B, it is shown that damping is so small at the high altitudes where the trajectory deflection occurs, that it has a negligible effect on the dispersion.

Summary and Conclusions

A simple relation has been derived for the prediction of cross-range dispersion of a ballistic re-entry vehicle that is caused by an initial angular misalignment between the vehicle

Table 1 Altitude of trajectory deflection

K	h_l, kft	CR/θ_0, ft/rad
0.5	264	56.9
1.0	255	110
2.0	245	212
4.0	234	403
8.0	221	763

axis of symmetry and the velocity vector at entry. The dispersion is strongly dependent on the exoatmospheric attitude and motion, which determines the endoatmospheric lift vector precession behavior. Symmetric coning about the velocity vector (positive precession) results in small dispersion relative to the initially nonprecessing vehicle at angle of attack (which results in negative precession). Based on idealized first-order aerodynamics, dispersion is found to be relatively insensitive to all aerodynamic coefficients except static stability. This is the case because the initial lift nonaveraging occurs at high altitude before the vehicle has experienced appreciable drag deceleration and before aerodynamic damping has had an appreciable influence on the angle-of-attack convergence. Also, the lift force coefficient, which determines the lateral acceleration for a given angle of attack, influences the rate of angle-of-attack convergence for a given static margin, and there is a compensating effect in the lift nonaveraging process that minimizes the influence of this parameter on dispersion. Other significant results of the analysis are as follows:

1) Trajectory deflection occurs in a plane that leads the plane of the initial angular misalignment by approximately 90 deg.

2) Dispersion is approximately proportional to roll rate in contrast to lift nonaveraging dispersion from body-fixed configurational asymmetries, which is inversely proportional to roll rate.

3) Dispersion is essentially independent of vehicle mass properties with the exception of the radius of gyration in roll.

4) Dispersion is directly proportional to the angular misalignment and inversely proportional to static margin and $u\sin\gamma$.

Appendix A: Average Value of the Dispersion Integral

We wish to find the average value of the integral

$$\mathcal{I} = -iK\int_l^X \sqrt{x}\exp\{iK[\ell n(1+x) - x + 1 - \ell n\, 2]\}\,dx \qquad \text{(A1)}$$

as X becomes large. Consider first the real part of $\mathcal{I}$ and make the change of variable

$$y = x - 1 \qquad \text{(A2)}$$

such that

$$v = \mathrm{Re}\mathcal{I} = K\int_0^Y \sqrt{1+y}\,\sin K\left[\ell n\left(1+\frac{y}{2}\right) - y\right]dy \qquad \text{(A3)}$$

We define the average value of v as occurring where $v''(y) = 0$, as shown in Fig. A1. From Eq. (A3), $v'(y)$ is defined by

$$v'(y) = f(y)\sin\psi(y) \qquad \text{(A4)}$$

and the average values of $v(y)$ occur at $y = y_n$ where

$$v''(y_n) = f'(y_n)\sin\psi(y_n) + f(y_n)\psi'(y_n)\cos\psi(y_n) = 0$$

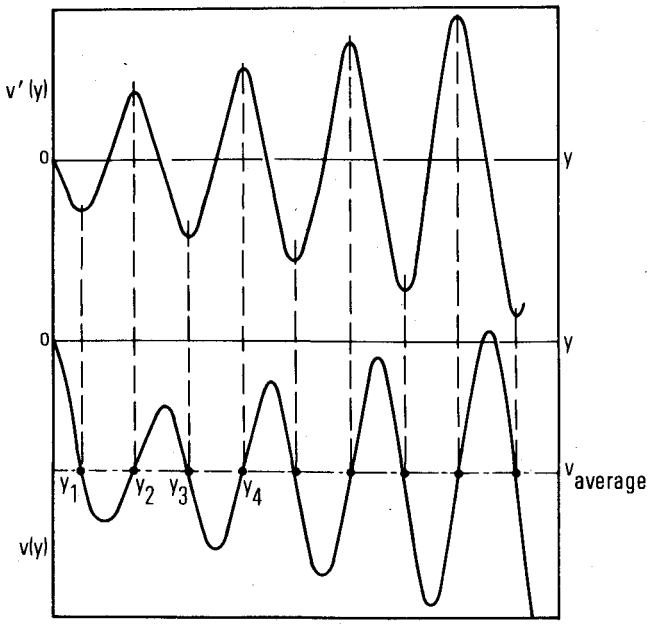

Fig. A1 Average value of the function $v(y)$.

or

$$\tan\psi(y_n) = -f(y_n)\psi'(y_n)/f'(y_n) \tag{A5}$$

With $f(y) = K\sqrt{1+y}$ and $\psi(y) = K[\ln(1+y/2) - y]$ from Eq. (A3), Eq. (A5) becomes

$$\tan\psi(y_n) = \tan K[\ln(1+y_n/2) - y_n]$$

$$= \frac{2K(1+y_n)^2}{2+y_n} \tag{A6}$$

For K sufficiently large, the right side of Eq. (A6) is positive and $\gg 1$ such that the angles $\psi(y_n)$ must lie in the first and fourth quadrants near $\pm\pi/2$

$$\psi(y_n) = -[(2n-1)\pi/2 + \mu_n] \qquad (n = 1,2,3,\ldots) \tag{A7}$$

where μ_n is a small angle. Substitution of this value in Eq. (A6) and the use of the identity for the tangent of a sum yields

$$\tan\psi(y_n) = \frac{1}{\tan\mu_n} = \frac{2K(1+y_n)^2}{2+y_n} \tag{A8}$$

or, since μ_n is small,

$$\tan\mu_n \approx \mu_n = \frac{2+y_n}{2K(1+y_n)^2} \tag{A9}$$

The values of the precession angle $\psi(y_n)$ where the average values of v occur are then, from Eq. (A7),

$$\psi(y_n) = K[\ln(1+y_n/2) - y_n]$$

$$= -\left[\frac{(2n-1)\pi}{2} + \frac{2+y_n}{2K(1+y_n)^2}\right] \tag{A10}$$

We can obtain approximate expressions for $\psi(y_n)$ and for y_n by using the series expansion for the $\ln$ term

$$\ln\left(1+\frac{y_n}{2}\right) = \frac{y_n}{2}\left[1 - \frac{1}{2}\left(\frac{y_n}{2}\right)^2 + \frac{1}{3}\left(\frac{y_n}{2}\right)^3 - \ldots\right] \tag{A11}$$

If the first average point occurs at sufficiently small y_1, we can approximate $\ln(1+y_1/2)$ by the first term of the series. With this approximation and neglecting μ_1 relative to $\pi/2$ for sufficiently large K, we obtain from Eq. (A10)

$$y_1 = \pi/K \tag{A12}$$

The net transverse velocity from Eq. (A3) with the first-order approximation $\ln(1+y/2) \approx y/2$ is

$$v(y_1) = K\int_0^{y_1} \sqrt{1+y}\,\sin\left(-\frac{Ky}{2}\right)dy$$

$$\approx -2\int_0^{\pi/2} \sin\left(\frac{Ky}{2}\right)d\left(\frac{Ky}{2}\right)$$

$$= -2 \tag{A13}$$

where we have neglected y relative to unity in the square-root term. For subsequent values of y_n sufficiently small that the approximations that contribute to the result of Eq. (A13) are valid, there would be no change in the subsequent average values because

$$\Delta v_{y_n - y_{n+1}} = -2\int_{(2n-1)\pi/2}^{(2n+1)\pi/2} \sin\left(\frac{Ky}{2}\right)d\left(\frac{Ky}{2}\right) = 0 \tag{A14}$$

It can be shown by a procedure similar to that described above that the imaginary component of $\mathcal{I}$ is zero for all sufficiently large K. Hence, the average value of the integral $\mathcal{I}$ is

$$\bar{\mathcal{I}} = \bar{v} + i\bar{w} = -2 \tag{A15}$$

which is independent of K for sufficiently large K.

Appendix B: Effect of Damping on Dispersion

If aerodynamic damping is included in the equations of motion, Eqs. (2) and (3), we can write the damping moment derivatives $M_{\dot\theta}$ and $M_{\dot\psi}$ in the form

$$M_{\dot\theta} \approx M_{\dot\psi} = -\nu \tag{B1}$$

where

$$\nu \approx (\rho u S/2m)\,[C_{N_\alpha} - (md^2/2I)\,(C_{m_q} + C_{m_{\dot\alpha}})] \tag{B2}$$

The inclusion of damping does not alter the quasisteady approximation for precession rates, Eqs. (8) and (11), but it does influence the angle-of-attack convergence in the form[3]

$$\theta/\theta_0 \approx (1+\xi)^{-1/4}\exp(-b\xi) = x^{-1/2}\exp[-b(x^2-1)] \tag{B3}$$

where

$$b \approx \frac{p_r^2 IH}{2u^2 m x_{st}\sin\gamma}\left[1 - \frac{md^2}{2I}\left(\frac{C_{m_q} + C_{m_{\dot\alpha}}}{C_{N_\alpha}}\right)\right] \tag{B4}$$

The dispersion integral, Eq. (22), then has the factor $\exp[-b(x^2-1)]$ included in the integrand

$$\mathcal{I} = -iK\int_1^X \sqrt{x}\exp[-b(x^2-1)]\exp[i\Delta\psi(x)]\,dx \tag{B5}$$

The damping is so small at the high altitudes where the net trajectory deflection occurs, that the added term has a negligible effect on the value of the integral in Eq. (B5). This becomes apparent if we change the independent variable to y defined in Eq. (A2), which gives

$$\mathcal{I} = -iK\int_0^Y \sqrt{1+y}\exp[-by(y+2)]\exp[i\psi(y)]\,dy \tag{B6}$$

It was shown in Appendix A that, for sufficiently large K, the first average of ϑ occurs at $y=y_1$, where $y_1 \ll 1$. For example, from the vehicle and trajectory parameters listed in the Analysis section with $C_{m_q}+C_{m_{\dot{\alpha}}}=-5$, the coefficient b is found to have the value $b=2.05\times 10^{-4}$. Thus, the damping term $\exp[-by(y+2)]$ remains essentially unity over the integration limits and would change insignificantly even for an order of magnitude increase in the damping derivative $C_{m_q}+C_{m_{\dot{\alpha}}}$.

Acknowledgments

This work was supported by the U.S. Air Force under Space and Missile Systems (SAMSO) Contract No. F04701-77-C-0078. The author is grateful to B.A. Troesch of the University of Southern California for his helpful suggestions for evaluating the intergral in Appendix A, to N.W. Oberholtzer of General Electric's Re-entry and Environmental Systems Division for reviewing the manuscript and pointing out an error in Eq. (24) and the approximation Eq. (26), and to M.E. Brennan for performing the numerical computations.

References

[1] Pettus, J.J., Larmour, R.A., and Palmer, R.H., "A Phenomenological Framework for Re-entry Dispersion Source Modeling," AIAA Paper 77-1152, AIAA Atmospheric Flight Mechanics Conference, Hollywood, Fla., Aug. 8-10, 1977.

[2] Platus, D.H., "Dispersion of Spinning Missiles Due to Lift Nonaveraging," *AIAA Journal*, Vol. 15, July 1977, pp. 909-915.

[3] Platus, D.H., "Angle-of-Attack Convergence and Windward-Meridian Rotation Rate of Rolling Reentry Vehicles," *AIAA Journal*, Vol. 7, Dec. 1969, pp. 2324-2330.